

JCTC

Journal of Chemical Theory and Computation

Lowest-Lying Conformers of Alanine: Pushing Theory to Ascertain Precise Energetics and Semiexperimental R_e Structures

Heather M. Jaeger,[†] Henry F. Schaefer III,[†] Jean Demaison,[‡] Attila G. Császár,^{*,§} and Wesley D. Allen^{*,†}

Center for Computational Chemistry and Department of Chemistry, University of Georgia, Athens, Georgia 30602, Laboratoire de Physique des Lasers, Atomes et Molécules, UMR CNRS 8523, Université de Lille I, 59655 Villeneuve d'Ascq Cedex, France, and Laboratory of Molecular Spectroscopy, Institute of Chemistry, Eötvös University, H-1518 Budapest 112, P.O. Box 32, Hungary

Received January 12, 2010

Abstract: The two lowest-energy gas-phase conformers, **Ala-I** and **Ala-IIA**, of the natural amino acid L-alanine (Ala) have been investigated by means of rigorous ab initio computations. Born–Oppenheimer (BO) equilibrium structures (r_e^{BO}) were fully optimized at the coupled-cluster [CCSD(T)/cc-pVTZ] level of electronic structure theory. Corresponding semiexperimental (SE) equilibrium structures (r_e^{SE}) of each conformer were determined for the first time by least-squares refinement of 11–15 structural parameters on modified, experimental rotational constant data from 10 isotopologues. The SE equilibrium rotational constants were obtained by, first, refitting Fourier transform microwave spectra using the method of predicate observations and, second, correcting the resulting effective rotational constants with theoretical vibration–rotation interaction constants (α_i). Careful analysis is made of the procedures to account for vibrational distortion, which proves essential to defining precise structures in flexible molecules such as Ala. Because Ala possesses no symmetry, has several large-amplitude nuclear motions, and exhibits conformers with different hydrogen bonding patterns, it is one of the most difficult cases where reliable equilibrium structures have now been determined. The relative energy of the alanine conformers was pinpointed using first-principles composite focal point analyses (FPA), which employed extrapolations using basis sets as large as aug-cc-pV5Z and electron correlation treatments as extensive as CCSD(T). The FPA computations place the **Ala-IIA** equilibrium structure higher in energy than that of **Ala-I** by a mere 0.45 kJ mol⁻¹ (38 cm⁻¹), showing that the two lowest-lying conformers of alanine are nearly isoenergetic; inclusion of zero-point vibrational energy increases the relative energy to 2.11 kJ mol⁻¹ (176 cm⁻¹). The yet unobserved **Ala-IIB** conformer is found to be separated from **Ala-IIA** by a vibrationally adiabatic isomerization barrier of only 16 cm⁻¹.

I. Introduction

Flexible molecules have potential energy surfaces (PESs) characterized by flat regions and low barriers for conforma-

tional isomerization.^{1–3} L-Alanine (Ala) and all other natural amino acids exhibit such characteristics and have a sizable number of low-energy conformers.^{4–19} The primary differences between the conformers of gas-phase amino acids, which exist exclusively in neutral form, are the number and types of intramolecular hydrogen bonds occurring for various configurations of the amino, carboxylic acid, and any polar side-chain groups. In the case of Ala, the dihedral angle about the central carbon–carbon bond, $\tau(\text{O}=\text{C}-\text{C}_\alpha-\text{N})$, remains

* To whom correspondence should be addressed. E-mail: wdallen@uga.edu (W.D.A.); csaszar@chem.elte.hu (A.G.C.).

[†] University of Georgia.

[‡] Université de Lille.

[§] Eötvös University.

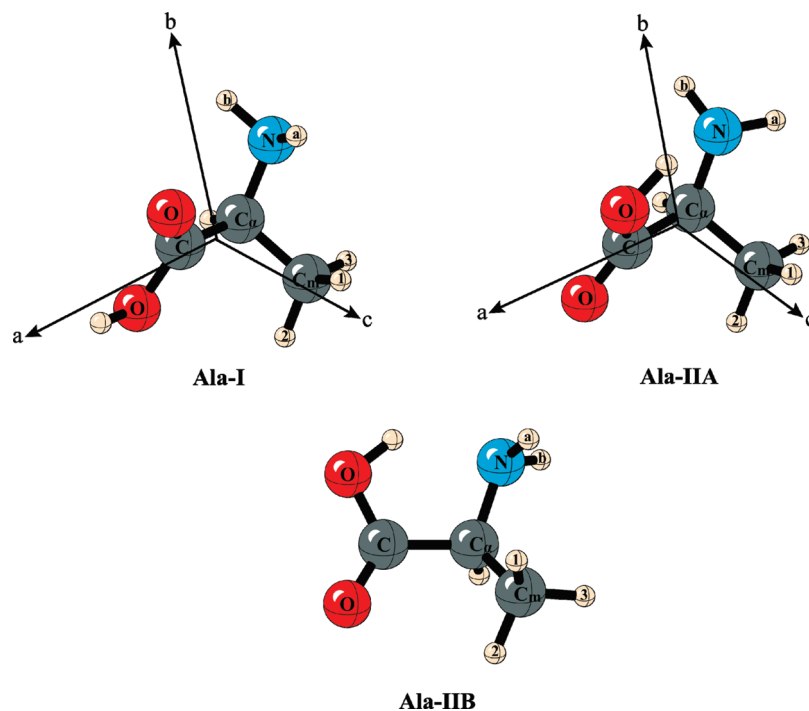


Figure 1. L-Alanine conformers **I**, **IIA**, and **IIB**.

consistently near 0° or 180° for all conformers, despite the variety of possible hydrogen bonds.

Experiments on the structure(s) of free Ala have included gas-phase electron diffraction (GED),^{11,12} jet-cooled millimeterwave (MMW) and Fourier transform microwave (FTMW) spectroscopy in molecular beams,^{5,9,10} and matrix-isolation infrared spectroscopy.¹³ The GED results for Ala cannot provide a clear distinction between the multiple conformers present at the elevated temperature of the experiments. Moreover, the derived r_g , r_α , and r_α^0 structural parameters differ substantially from the corresponding equilibrium (r_e) values because of temperature-dependent rotational–vibrational effects, which can be as large as those induced by conformational changes. The low-temperature MMW and FTMW molecular beam experiments^{5,9,10} clearly identified two gas-phase conformers, **Ala-I** and **Ala-IIA** (Figure 1). The failure to observe other low-energy conformers given by electronic structure computations^{4,6–8} has been attributed to vibrational relaxation in the free-jet expansions.²⁰ The matrix-isolation infrared experiments¹³ also observed two conformers of alanine.

Select r_0 and r_s parameters for **Ala-I** and **Ala-IIA** have been determined⁵ from two sets of FTMW rotational constants involving 10 isotopologues of each conformer. Unfortunately, this approach is not sufficient to obtain an accurate, well-defined empirical structure. Equilibrium structures, free from undesirable isotopic, rotational–vibrational, and temperature effects, are often difficult, if not impossible, to obtain experimentally, especially for flexible molecules. Vibrational distortion, arising from flat, anharmonic regions on the PES, can greatly influence the effective, experimental rotational constants, leading to sizable isotopic effects even at low temperature. Consequently, for conformers of flexible molecules, only equilibrium structures can be compared to one another with any degree of validity. For example,

differences between the backbone structures of glycine and alanine should be ascertained from r_e parameters (see Section III.F).

A protocol has been established whereby a semiexperimental equilibrium structure (r_e^{SE}) can be determined by first correcting empirical, effective ground-state rotational constants with ab initio vibration–rotation interaction constants (α_i) and then performing a structural refinement on the resulting “experimental” equilibrium rotational constants (B_e^{SE}).²¹ This combined experimental and theoretical approach has been successfully applied in many studies,^{21–34} including work that has given r_e^{SE} structures for the lowest-energy conformers of the neutral amino acids glycine (Gly)²⁴ and proline (Pro).²³ In this investigation, accurate r_e^{SE} structures of **Ala-I** and **Ala-IIA** are determined after refitting spectroscopic constants to the observed rotational transitions,⁵ deriving B_e^{SE} constants for 10 isotopologues of each conformer, and imposing geometric constraints from Born–Oppenheimer equilibrium structures (r_e^{BO}) obtained at the highest feasible level of ab initio electronic structure theory [CCSD(T)/cc-pVTZ, vide infra]. This is the first study to conjoin theory and experiment to derive reliable equilibrium structures, including detailed error analyses for both theoretical and experimental procedures, for a molecule as large and flexible as Ala.

All low-energy conformers of Ala possess intramolecular hydrogen bonds that significantly stabilize these structures, increase their rigidity, and provide challenges for electronic structure theory, as shown in numerous previous ab initio studies.^{1,7,14,35–37} The sensitivity of Ala conformational energies to the level of electronic structure theory has been demonstrated by Császár,^{1,7} and Figure 2 vividly displays the energetic variations observed⁷ for **Ala-I**, **Ala-II(A/B)**, and **Ala-III(A/B)**. The **Ala-III** conformers are derived from the **Ala-I** structure in Figure 1 by a 180° rotation of the

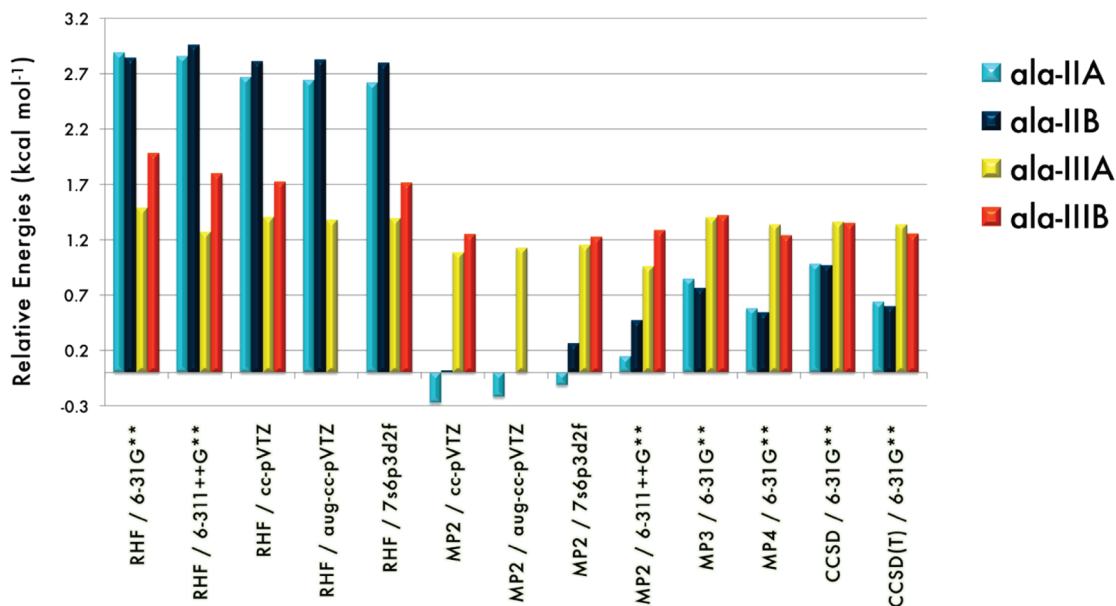


Figure 2. Equilibrium energies relative to **Ala-I** at various levels of electronic structure theory.

–COOH moiety about the C–C_α bond, the two variants differing in whether the carboxyl O–H bond is oriented toward (**IIIA**) or away from (**IIIB**) the methyl substituent at C_α.⁷ Electron correlation reverses the energy ordering of **Ala-II(A/B)** and **Ala-III(A/B)**, in accord with known deficiencies of Hartree–Fock theory in predicting conformational energies of amino acids.^{1,14,38} Strong basis set dependence of conformational energies is also exhibited; large basis sets with diffuse functions are necessary to fully capture the differences in intramolecular hydrogen bonding interactions. In this work, the relative energy of **Ala-IIA** with respect to **Ala-I** in the nonrelativistic, ab initio limit is determined by applying the composite focal point analysis (FPA) approach^{39–44} that has been used successfully in previous studies on amino acids^{1,7,8,14,23,24} and many other species.^{40,43,45–50}

II. Computational Methods

II.A. Semiexperimental Equilibrium Structures. The derivation of r_c^{SE} structures involves three main steps: optimization of reliable r_c^{BO} structures, computation of an ab initio cubic force field with subsequent evaluation of α_i constants to extract equilibrium B_c^{SE} parameters from the experimental rotational constants, and a tight least-squares structural fit to selected B_c^{SE} values for several isotopologues, incorporating r_c^{BO} constraints as necessary. In this study, the r_c^{BO} geometries of **Ala-I** and **Ala-IIA** were fully optimized using frozen-core (FC) CCSD(T) coupled-cluster theory^{51–53} paired with the correlation-consistent cc-pVTZ basis set of [4s3p2d1f] and [3s2p1d] quality for {C, N, O} and H, respectively.⁵⁴ While the inclusion of core electron correlation during these demanding geometry optimizations was not feasible, the corresponding effects⁵⁵ on the r_c^{BO} parameters are expected to lie within the uncertainties of most r_c^{SE} parameters and are partially corrected during the least-squares fit. Geometry optimizations were carried out in natural internal coordinates^{56,57} using a quasi-Newton–Raphson method implemented in the PSI3 package.⁵⁸ The optimization

of highly flexible coordinates was facilitated with a fixed Hessian matrix evaluated at the MP2 level with a (9s5p) double- ζ valence basis set⁵⁹ (DZ) at a point near the target minimum. Energy gradients were computed by finite differences of energies provided by the MOLPRO⁶⁰ package using a five-point central difference formula to ensure numerical accuracy for both high- and low-frequency modes. Finally, minima were verified by evaluating the molecular gradients analytically using the MAB-ACESII⁶¹ program. Cartesian coordinates of the CCSD(T)/cc-pVTZ r_c^{BO} structures of **Ala-I** and **Ala-IIA** are provided in Supporting Information (Table S1).

For both conformers of Ala, anharmonic force fields were determined at the all-electron MP2/6-31G(d)⁶² level at the corresponding minima to avoid the nonzero force dilemma.⁶³ The cubic and semidiagonal quartic force constants in normal coordinates were evaluated by numerical differentiation of analytically computed second derivatives. Built-in features⁶⁴ of MAB-ACESII then gave the vibration–rotation interaction constants for all isotopologues according to the second-order vibrational perturbation theory⁶⁵ (VPT2) formula

$$\alpha_i^B = -\frac{2B_c^2}{\omega_i} \left[\sum_{\xi=a,b,c} \frac{3(a_i^{b\xi})^2}{4I_\xi} + \sum_{j(\neq i)} (\zeta_{ij}^b)^2 \frac{(3\omega_i^2 + \omega_j^2)}{\omega_i^2 - \omega_j^2} + \pi \left(\frac{c}{h}\right)^{1/2} \sum_j \phi_{ij} a_j^{bb} \left(\frac{\omega_i}{\omega_j^{3/2}}\right) \right] \quad (1)$$

in which indices (i, j) denote normal coordinates (Q_i, Q_j) with harmonic vibrational frequencies (ω_i, ω_j), I_ξ is a principal moment of inertia, $a_i^{b\xi}$ is a first derivative of inertial tensor element $I_{b\xi}$ with respect to Q_i , ζ_{ij}^b is a Coriolis coupling constant, and ϕ_{ij} is a cubic force constant in the reduced normal coordinate space. In lowest-order and without centrifugal distortion corrections, the effective ground-state rotational constants (B_0) are related to their equilibrium counterparts by the expression

$$B_e - B_0 = \frac{1}{2} \sum_i \alpha_i^B = -B_e^2 \left[\frac{3}{4} \sum_{i\xi} \frac{(a_i^{b\xi})^2}{\omega_i^2 I_\xi} - \sum_{i<j} \frac{(\zeta_{ij}^b)^2 (\omega_i - \omega_j)^2}{\omega_i \omega_j (\omega_i + \omega_j)} + \pi \left(\frac{c}{h}\right)^{1/2} \sum_{ij} \phi_{ij} a_j^{bb} \omega_j^{-3/2} \right] \quad (2)$$

which was employed in this study to obtain semiexperimental B_e^{SE} constants. Note that all Coriolis resonance terms appearing in eq 1 are canceled in the reduced form on the right side of eq 2, an important point often not fully appreciated.

The weighted least-squares refinement^{66–68} for the r_e^{SE} structures employed linear combinations of simple valence internal coordinates and was carried out with the MolStruct⁶⁹ code. The weights were chosen as the reciprocal statistical uncertainties in the experimentally derived rotational constants. For both **Ala-I** and **Ala-IIA**, experimental data is available for ten isotopologues, yielding 30 B_e^{SE} constants each (Supporting Information, Table S2). However, not all of these constants proved suitable for the r_e^{SE} refinements. Because **Ala-I** and **Ala-IIA** possess no symmetry, the number of independent geometric parameters (33) is greater than the experimental data set, necessitating the use of r_e^{BO} structural constraints. The least-squares refinements were performed on select sets of internal coordinates and rotational constants. Within least-squares fits, the standard errors intrinsic to each variable and the deviations for the rotational constants were monitored carefully.

The success of the r_e^{SE} procedure depends on the number of isotopologues with accurate experimental rotational constants that can be used to determine meaningful structural parameters, the accuracy of the anharmonic force fields and theoretical α_i constants, the quality of the r_e^{BO} least-squares constraints, and the validity of modeling vibrational effects via first-order vibration–rotation interaction (eq 2). The utility of α_i constants suffers more from the inherent approximations within VPT2 for large, flexible molecules with highly anharmonic vibrational modes than for small, rigid molecules exhibiting predominantly harmonic motions and small rovibrational couplings. By employing eq 2, higher-order vibration–rotation interactions and centrifugal distortion are neglected, despite their enhanced significance for flexible molecules. Centrifugal distortion contamination appears in both the experimental rotational constants and the theoretical correction of B_0 to extract B_e^{SE} .⁷⁰ Thus, while the effective rotational constants of certain isotopologues may describe the observables accurately, caution must be exercised in using these constants to refine the semiexperimental structure.

II.B. Conformational Energetics. The method of focal point analysis (FPA)^{39–44} provides a means of systematically approaching and monitoring convergence of ab initio computations toward the one-particle complete basis set (CBS) limit and the fully correlated many-electron wave function (full configuration interaction, FCI). In this study, an FPA investigation of the **Ala-IIA–Ala-I** relative energy was executed with correlation-consistent basis sets augmented with diffuse functions,^{54,71} aug-cc-pVXZ (X = D, T, Q, 5). Hartree–Fock (X = T, Q, 5) and MP2 (X = Q, 5) energies

were extrapolated to the CBS limit using standard exponential and inverse cubic formulas, respectively.^{72,73} Higher-order correlation effects were incorporated by means of additive CCSD/aug-cc-pVQZ and CCSD(T)/aug-cc-pVTZ increments. Core correlation was included by appending the difference between all-electron and frozen-core CCSD(T)/cc-pCVTZ results to the valence FPA limit. The frozen-core CCSD(T)/cc-pVTZ r_e^{BO} geometries were adopted as reference structures in the FPA computations.

The zero-point vibrational energies (ZPVEs) of **Ala-I** and **Ala-IIA** were first computed from the MP2/6-31G(d) anharmonic force fields via the expression

$$\text{ZPVE} = \frac{1}{2} \sum_i \omega_i + \frac{1}{4} \sum_{i \leq j} \chi_{ij} \quad (3)$$

where χ_{ij} denotes the second-order vibrational anharmonicity constants derived from VPT2.⁶⁵ The effect of anharmonicity on the ZPVE correction (Δ_{ZPVE}) to the **Ala-IIA–Ala-I** energy separation was less than 0.02 kJ mol^{−1}. Therefore, our final Δ_{ZPVE} value (+1.66 kJ mol^{−1}) was evaluated from harmonic vibrational frequencies computed at the highest feasible level of theory, all-electron MP2 with a pared aug-cc-pVTZ basis set.⁷⁴

III. Results and Discussion

III.A. Lowest-Energy Conformers of Ala. Extensive conformational searching for Gly¹⁴ and Ala,^{4,6,7} the two smallest amino acids, has revealed 8 and 13 distinct conformers, respectively. An unmistakable correspondence exists between the Gly and Ala conformers because both have inert side groups (−H for Gly, −CH₃ for Ala) leading to the same intramolecular hydrogen bonding possibilities. A bifurcated hydrogen bond forms between the carbonyl oxygen atom and the amino hydrogen atoms in the global minima **Gly-I** and **Ala-I**. Upon ~180° rotation of the −COOH plane, hydrogen bonding occurs with −OH as the proton donor and −NH₂ as the acceptor, resulting in the **Gly-IIa** and the **Ala-II** conformers. The suffix in the **Gly-IIa** designation indicates a *non*-planar backbone, although accurate FPA computations find a barrier to planarity of only 21 ± 5 cm^{−1}.²⁴ The two Ala structures corresponding to **Gly-IIa** exist as a nearly isoenergetic pair, **Ala-IIA** and **Ala-IIB**, having the same H-bonding arrangement but different orientations of the methyl group (Figure 1). **Ala-I** has repeatedly been observed as the predominant conformer in the rotational spectra of alanine,^{5,9,10} in accord with high-level theoretical results. In fact, large basis CCSD, CCSD(T), and MP4 single-point energy computations at MP2/6-311++G** optimum geometries determine **Ala-I** to be more stable than the **Ala-II** conformers by 200–300 cm^{−1}.⁷ The same levels of theory predict that the next conformers (**Ala-III**) are, again, 200–300 cm^{−1} higher in energy than the **Ala-II** conformers. While the **Ala-I** and **Ala-IIA** conformers were identified^{5,9} in the observed rotational spectra by ¹⁴N nuclear quadrupole coupling, **Ala-IIB** and higher-energy conformers were never observed.

Prior speculation on the absence of **Ala-IIB** in the observed rotational spectra was based on a presumably low

interconversion barrier for **Ala-IIB** \rightarrow **Ala-IIA**. To elucidate this issue, we computed CCSD(T) energy points with the aug-cc-pVTZ basis set at the MP2/6-311++G(d,p) stationary structures of **Ala-IIA**, **Ala-IIB**, and the connecting transition state optimized in this work. The resulting well depth of **Ala-IIB** with respect to the interconversion barrier is only 34 cm^{-1} , which is reduced to a minuscule 16 cm^{-1} upon vibrational correction. To obtain this vibrationally adiabatic barrier, MP2/cc-pVTZ harmonic frequencies were computed, and ZPVEs were evaluated by excluding at each stationary point the contribution from the normal mode connecting **Ala-IIA** to **Ala-IIB**. In summary, the small amount of energy required to interconvert the **Ala-II** conformers is indeed representative of the conformational flexibility of Ala and may rationalize the absence of **Ala-IIB** in the molecular beam experiments.^{20,75,76}

III.B. Refitting the Rotational Spectra of Ala. Before determining r_c^{SE} structures, we refit the existing rotational spectra of alanine to more firmly establish the rotational constants and their uncertainties for the structural analysis. In the original spectroscopic study,⁵ the rotational, centrifugal distortion, and nuclear quadrupole hyperfine constants of alanine were simultaneously determined from a global fit of a chosen Hamiltonian to the measured transitions. From a statistical point of view, this method is meritorious and has the advantage of being simple. However, overly optimistic uncertainties are produced when the data set for the global fit is small, as is the case here. Moreover, from a numerical perspective, correlations are induced between the centrifugal distortion constants and the remaining rotational parameters, worsening the condition number.⁷⁷ Finally, “masked” errors that do not yield outlying residuals become more prevalent.⁷⁸ For these reasons, we first corrected the transitions for the nuclear quadrupole hyperfine structure and then fit the hypothetical unperturbed rotational transitions to a standard Watson Hamiltonian.⁷⁹ It could be argued that this approach might give biased rotational parameters containing systematic errors due to inaccuracies in the nuclear quadrupole hyperfine constants. However, when several hyperfine components of the same rotational transition are measured, as for a great majority of the reported transitions,⁵ the hypothetical, unperturbed frequencies may be calculated using the intensity-weighted mean of the multiplets.⁸⁰ As a consequence, accurate knowledge of the nuclear quadrupole hyperfine constants is unnecessary and the possible contribution of the spin-rotation interaction is canceled. Furthermore, our approach permits the elimination of outliers, the estimation of the uncertainty of the measurements, and an increase in the reliability of the rotational frequencies.

Another issue in the original fits⁵ is that the full set of quartic centrifugal distortion constants was not determinable for many isotopologues, and hence these constants were fixed to values for the parent (or ¹⁵N) species. Our computations revealed significant variations in the centrifugal distortion constants from one isotopologue to another (vide infra). Therefore, we used the method of predicate observations⁸¹ in our refitting, in which the ab initio “scaled” centrifugal distortion constants (or the constants of another isotopologue) are input data in a weighted least-squares fit. Though this

method permits the approximate determination of the centrifugal distortion constants, it must be used with care, and it is essential to check that the derived constants are really compatible with the experimental data. In our fits the weights of the predicate observations were varied to keep the corresponding “jackknifed” residuals, $t(i)$, small (typically less than 3), where $t(i)$ is the i th residual divided by its standard deviation calculated by omitting the i th transition.⁷⁸

Parent values and isotopic shifts for the effective rotational constants and quartic centrifugal distortion constants of the **Ala-I** and **Ala-IIA** isotopologues are reported in Tables 1 and 2, respectively. Three sets of data are tabulated: our results from refitting the observed lines (refit), our CCSD(T)/cc-pVTZ theoretical values (theor), and the original experimental constants (expt).⁵ Rotational constant shifts associated with heavy-atom (non-hydrogen) isotopic substitution exhibit modest differences (2–5 kHz) between original and refit values and are relatively independent of the method used to fit the rotational spectra. However, much larger deviations are found between the original and refit values for many of the D-substituted isotopologues. The largest discrepancies (in kHz) are 868 for B_0 of O–D (**Ala-I**), 476 for A_0 of C_m-3D (**Ala-IIA**), 84 for A_0 of N–D_a (**Ala-I**), 47 for A_0 of N–D_a (**Ala-IIA**), and 46 for B_0 of C_m-3D (**Ala-IIA**). Comparing these discrepancies to the average residual of the structural fits for Ala and Gly, around 20 kHz (ref 24 and below), it becomes clear that these rotational constants should not be given much weight in the determination of r_c^{SE} structures.

The theoretical isotopic shifts (Tables 1 and 2) are based on (A_0 , B_0 , C_0) constants, which are determined by conjoining our MP2/6-31G(d) vibration–rotation interaction constants and CCSD(T)/cc-pVTZ equilibrium rotational constants (B_e^{BO}). The theoretical and experimental heavy-atom isotopic shifts of the (A_0 , B_0 , C_0) constants are generally in remarkable agreement. The mean absolute deviations between refit and theor isotopic shifts among the (¹³C, ¹³C_α, ¹³C_m, ¹⁵N) isotopologues are 0.2 and 0.4 MHz in the **Ala-I** and **Ala-IIA** cases, respectively. On the other hand, most isotopic-shift disparities for the deuterated isotopologues are greater than 1 MHz. The proximity of the D_b position to the methyl group seems to enhance the error in the vibrationally corrected rotational constants of the N–D_b isotopologue, especially in comparison to N–D_a. The two largest absolute discrepancies are (8.7, 3.5) MHz for [A_0 (**Ala-IIA**), B_0 (**Ala-I**)] of the triply deuterated methyl isotopologues, C_m-3D . Nevertheless, on a percentage basis, the discord between the refit and theor isotopic shifts is less than 2% even in these instances. For the centrifugal distortion constants, the refit and theor isotopic shifts agree quite well for **Ala-I**, similarly to other molecules.^{82,83} However, considerable differences occur for the Δ_{JK} , Δ_K , and δ_K isotopic shifts of **Ala-IIA**. The underlying cause is not transparent and is not specific to the deuterated isotopologues.

Relevant to the structure refinements, the number of fitted transitions for the ¹⁵N isotopologues of **Ala-I** and **Ala-IIA** is relatively small. This is particularly true in the **Ala-IIA** case, where 17 lines were used to determine 8 parameters (3 rotational and 5 quartic centrifugal distortion constants).

Table 1. Isotopic Shifts of Effective Rotational Constants (A_0 , B_0 , C_0) and A-Reduced Quartic Centrifugal Distortion Constants (Δ_J , Δ_{JK} , Δ_K , δ_J , δ_K) for **Ala-I**: Original Experimental Constants from Ref 5 (expt), Current Refitting of Observed Lines (refit), and CCSD(T)/cc-pVTZ Theoretical Values (theor)^a

constant	parent	¹³ C	¹³ C _α	¹³ C _m	¹⁵ N	C _α -D	C _m -3D	O-D	N-D _a	N-D _b	MAD	
A_0 expt	5066.1456(4)	-0.941	-8.821	-95.254	-48.851	-113.253	-462.026	-13.968	-104.850	-176.847		
	refit	5066.1455(7)	-0.941	-8.821	-95.254	-48.851	-113.250	-462.025	-13.965	-104.934	0.777	
	theor	5031.4685	-0.939	-8.995	-94.714	-48.400	-112.952	-459.265	-12.775	-104.774	-175.431	
B_0 expt	3100.9506(3)	-9.668	-12.419	-33.767	-50.457	-51.813	-175.397	-109.991	-57.095	-49.805		
	refit	3100.9507(5)	-9.667	-12.421	-33.767	-50.458	-51.818	-175.404	-110.859	-57.103	-49.804	1.347
	theor	3067.4442	-9.505	-12.209	-33.324	-50.093	-50.240	-171.944	-109.247	-54.348	-48.269	
C_0 expt	2264.0134(2)	-5.178	-5.343	-31.628	-34.806	-5.462	-141.514	-61.745	-41.615	-45.195		
	refit	2264.0131(4)	-5.178	-5.342	-31.628	-34.806	-5.458	-141.510	-61.749	-41.608	-45.197	0.307
	theor	2258.8416	-5.199	-5.370	-31.518	-34.921	-6.150	-141.609	-61.727	-40.245	-44.884	
Δ_J expt	2.452	-0.035	-0.029	-0.069	-0.121	-0.026	0	0	0	0		
	refit	2.445(7)	-0.024	-0.086	-0.072	-0.113	-0.138	-0.312	-0.262	-0.281	0.007	0.033
	theor	2.409	-0.027	-0.040	-0.042	-0.100	-0.195	-0.325	-0.245	-0.262	0.108	
Δ_{JK} expt	-6.391	0.052	0	0.324	0.112	0	0	0	0	0		
	refit	-6.38(1)	0.03	0.45	0.29	0.11	0.74	1.61	0.69	0.77	-0.74	0.08
	theor	-6.373	0.104	0.127	0.292	0.126	0.590	1.613	0.634	0.694	-0.741	
Δ_K expt	5.410	0.022	0	-0.21	0.124	0	0	0	0	0		
	refit	5.37(5)	0.07	-0.09	-0.18	0.15	-0.69	-1.55	-0.28	-0.36	0.53	0.08
	theor	5.424	-0.077	-0.114	-0.298	-0.032	-0.568	-1.570	-0.324	-0.413	0.478	
δ_J expt	0.5696	0.0013	-0.0216	-0.0109	-0.0294	0	0	0	0	0		
	refit	0.574(2)	0.008	-0.028	-0.010	-0.033	-0.061	-0.094	-0.066	-0.084	0.058	0.009
	theor	0.570	-0.009	-0.014	-0.011	-0.023	-0.070	-0.095	-0.053	-0.077	0.064	
δ_K expt	10.3777	0.0083	0.2823	-0.4577	-0.3647	0.5423	0	0	0	0		
	refit	10.37(3)	0.07	-0.31	-0.36	-0.34	-0.71	-1.80	-0.11	-1.36	0.22	0.13
	theor	9.656	-0.025	-0.058	-0.297	-0.273	-0.775	-1.734	-0.303	-1.442	-0.042	

^a Units: MHz for (A_0 , B_0 , C_0) and kHz for (Δ_J , Δ_{JK} , Δ_K , δ_J , δ_K); MAD = mean absolute deviation between refit and theor isotopic shifts. Large deviations of theoretical and experimental rotational constants are italicized. The CCSD(T)/cc-pVTZ rotational constants include MP2/6-31G(d) vibrational corrections.

Table 2. Isotopic Shifts of Effective Rotational Constants (A_0 , B_0 , C_0) and A-Reduced Quartic Centrifugal Distortion Constants (Δ_J , Δ_{JK} , Δ_K , δ_J , δ_K) for **Ala-IIA**: Original Experimental Constants from Ref 5 (expt), Current Refitting of Observed Lines (refit), and CCSD(T)/cc-pVTZ Theoretical Values (theor)^a

constant	parent	¹³ C	¹³ C _α	¹³ C _m	¹⁵ N	C _α -D	C _m -3D	O-D	N-D _a	N-D _b	MAD	
A_0 expt	4973.0558(6)	-0.138	-10.402	-88.351	-54.385	-115.510	-441.476	-138.202	-35.075	-164.893		
	refit	4973.0546(35)	-0.136	-10.399	-88.356	-54.384	-115.537	-441.952	-138.198	-35.028	-164.887	2.566
	theor	4950.175	-0.177	-11.079	-88.826	-53.339	-117.566	-433.218	-134.674	-31.794	-168.219	
B_0 expt	3228.3379(5)	-12.458	-13.622	-39.366	-42.997	-54.464	-198.172	-8.122	-114.542	-77.573		
	refit	3228.3375(56)	-12.456	-13.622	-39.366	-42.997	-54.462	-198.218	-8.124	-114.543	-77.576	1.910
	theor	3183.801	-12.216	-13.218	-38.315	-42.527	-51.598	-195.056	-7.333	-113.036	-70.879	
C_0 expt	2307.8090(3)	-6.190	-5.382	-33.334	-31.976	-8.888	-148.755	-27.187	-61.942	-44.052		
	refit	2307.8090(42)	-6.191	-5.382	-33.333	-31.977	-8.890	-148.704	-27.182	-61.935	-44.047	0.858
	theor	2316.254	-6.326	-5.539	-33.356	-32.264	-10.313	-148.500	-26.600	-65.042	-45.800	
Δ_J expt	2.13(1)	0.038	-0.036	0.036	-0.004	-0.055	-0.004	-0.004	-0.004	-0.004		
	refit	2.11(6)	0.10	-0.02	0.09	0.01	-0.06	-0.06	-0.01	0.16	-0.01	0.09
	theor	1.397	-0.016	-0.022	-0.016	-0.055	-0.107	-0.152	0.016	-0.149	-0.086	
Δ_{JK} expt	-4.84(6)	-0.175	0.207	0.199	-0.358	-0.358	-0.358	-0.358	-0.358	-0.358		
	refit	-4.8(3)	-0.37	0.13	-0.03	-0.43	-0.18	-0.18	-0.27	-0.17	-0.25	0.37
	theor	-2.611	0.047	0.055	0.067	0.098	0.232	0.459	-0.100	0.306	0.279	
Δ_K expt	4.98(2)	0	0	0	0	-0.002	-0.002	-0.002	-0.002	-0.002		
	refit	4.6(5)	0.67	0.44	-0.63	0.43	0.42	0.42	0.44	0.43	0.43	0.64
	theor	2.772	-0.032	-0.069	-0.092	-0.058	-0.328	-0.574	0.009	-0.124	-0.390	
δ_J expt	0.41(1)	-0.010	-0.025	-0.015	-0.0087	-0.009	-0.009	-0.009	-0.009	-0.009		
	refit	0.41(2)	-0.01	-0.03	-0.04	-0.01	-0.01	-0.01	-0.01	-0.01	-0.01	0.02
	theor	0.257	-0.004	-0.006	-0.0002	-0.012	-0.033	-0.025	0.007	-0.023	-0.047	
δ_K expt	7.35(1)	0	0	0	0	0	0	0	0	0		
	refit	7.2(7)	0.59	0.11	0.26	0.15	0.97	0.97	-1.79	-1.68	-1.78	1.02
	theor	4.686	-0.008	-0.026	-0.172	-0.127	-0.388	-0.940	-0.320	-0.099	-0.317	

^a Units: MHz for (A_0 , B_0 , C_0) and kHz for (Δ_J , Δ_{JK} , Δ_K , δ_J , δ_K); MAD = mean absolute deviation between refit and theor isotopic shifts. Large deviations of theoretical and experimental rotational constants are italicized. The CCSD(T)/cc-pVTZ rotational constants include MP2/6-31G(d) vibrational corrections.

Accordingly, the standard deviation of the ¹⁵N(**Ala-IIA**) fit is only 0.2 kHz, less than 10% of the estimated experimental accuracy (3 kHz). For this reason, the standard deviations of the ¹⁵N parameters are perhaps one order of magnitude too small.

Highly anharmonic vibrational motions, such as the internal rotation of the methyl group, twisting along the backbone, or fluid rocking motion of the amino group, complicate the determination of vibrational corrections to

the effective experimental rotational constants. Fortunately, for isotopologues that exhibit similar vibrational effects as the parent, the error in the vibrational corrections is systematic and the least-squares refinement can still produce equilibrium structures with small standard errors. The statistical outliers (among the rotational constants) stem from isotopologues for which the substituted atom undergoes large-amplitude, anharmonic motion or yields large isotopic shifts. As such, isotopic substitutions at peripheral hydrogen

Table 3. Equilibrium Structures of **Ala-I**^a

parameters ^b	semiexperimental r_e			
	CCSD(T)/cc-pVTZ	Fit 1	Fit 2	Fit 3
$r(\text{C}-\text{C}_\alpha)$	1.5236	1.519(2)	1.518(2)	1.520(3)
$r(\text{C}_\alpha-\text{C}_m)$	1.5316	1.524(4)	1.526(3)	1.522(4)
$r(\text{C}_\alpha-\text{N})$	1.4570	1.446(4)	1.445(3)	1.448(4)
$r(\text{C}=\text{O})$	1.2085	1.208(6)	1.208(5)	1.207(7)
$r(\text{C}-\text{O})$	1.3551	1.347(5)	1.348(4)	1.349(6)
$r(\text{N}-\text{H})_{\text{Avg}}$	1.0156	1.0156	1.0156	1.014(4)
$\angle(\text{C}-\text{C}_\alpha-\text{C}_m)$	108.70	109.0(2)	108.8(2)	109.0(3)
$\angle(\text{C}-\text{C}_\alpha-\text{N})$	113.24	113.4(3)	113.5(3)	113.3(4)
$\angle(\text{C}_\alpha-\text{C}=\text{O})$	125.36	124.8(4)	126.1(4)	125.1(4)
$\angle(\text{O}-\text{C}=\text{O})$	122.81	122.7(1)	124.9(3)	122.7(2)
$\angle(\text{C}-\text{O}-\text{H})$	105.82	105.82	105.82	105.9(6)
$\angle(\text{C}-\text{C}_\alpha-\text{H})$	107.39	107.39	107.39	106.5(5)
$\tau(\text{O}-\text{C}-\text{C}_\alpha-\text{C}_m)$	-73.65	-71.9(3)	-71.8(3)	-71.9(4)
$\tau(\text{O}-\text{C}-\text{C}_\alpha-\text{H})$	43.98	43.98	43.98	47.5(9)
$\tau(\text{O}=\text{C}-\text{C}_\alpha-\text{N})$	-17.27	-16.2(5)	-16.1(4)	-16.2(8)

CCSD(T)/cc-pVTZ r_e^{BO} constraints			
$r(\text{O}-\text{H})$	0.9680	$\angle(\text{C}_\alpha-\text{C}_m-\text{H})_{\text{Diff1}}$	-0.54
$r(\text{C}_\alpha-\text{H})$	1.0925	$\angle(\text{C}_\alpha-\text{C}_m-\text{H})_{\text{Diff2}}$	2.02
$r(\text{N}-\text{H})_{\text{Diff}}$	0.0012	$\tau(\text{O}=\text{C}-\text{O}-\text{H})$	-0.90
$r(\text{C}_m-\text{H})_{\text{Avg}}$	1.0911	$\tau(\text{C}_\alpha-\text{C}-\text{O}-\text{H})$	177.80
$r(\text{C}_m-\text{H})_{\text{Diff1}}$	0.0075	$\tau(\text{C}-\text{C}_\alpha-\text{N}-\text{H}_a)$	54.01
$r(\text{C}_m-\text{H})_{\text{Diff2}}$	0.0007	$\tau(\text{C}-\text{C}_\alpha-\text{N}-\text{H}_b)$	-59.37
$\angle(\text{C}_\alpha-\text{N}-\text{H})_{\text{Avg}}$	108.66	$\tau(\text{H}-\text{C}_\alpha-\text{C}_m-\text{H}_1)$	180.86
$\angle(\text{H}_a-\text{N}-\text{H}_b)$	104.72	$\tau(\text{H}-\text{C}_\alpha-\text{C}_m-\text{H}_2)$	-58.90
$\angle(\text{C}_\alpha-\text{C}_m-\text{H})_{\text{Avg}}$	110.08	$\tau(\text{H}-\text{C}_\alpha-\text{C}_m-\text{H}_3)$	62.11

coordinate definitions	
$r(\text{N}-\text{H})_{\text{Avg}} = [r(\text{N}-\text{H}_a) + r(\text{N}-\text{H}_b)]/2$	
$r(\text{N}-\text{H})_{\text{Diff}} = [r(\text{N}-\text{H}_a) - r(\text{N}-\text{H}_b)]$	
$\angle(\text{C}_\alpha-\text{N}-\text{H})_{\text{Avg}} = [\angle(\text{C}_\alpha-\text{N}-\text{H}_a) + \angle(\text{C}_\alpha-\text{N}-\text{H}_b)]/2$	
$r(\text{C}_m-\text{H})_{\text{Avg}} = [r(\text{C}_m-\text{H}_1) + r(\text{C}_m-\text{H}_2) + r(\text{C}_m-\text{H}_3)]/3$	
$r(\text{C}_m-\text{H})_{\text{Diff1}} = 2[r(\text{C}_m-\text{H}_1)] - r(\text{C}_m-\text{H}_2) - r(\text{C}_m-\text{H}_3)$	
$r(\text{C}_m-\text{H})_{\text{Diff2}} = r(\text{C}_m-\text{H}_2) - r(\text{C}_m-\text{H}_3)$	
$\angle(\text{C}_\alpha-\text{C}_m-\text{H})_{\text{Avg}} = [\angle(\text{C}_\alpha-\text{C}_m-\text{H}_1) + \angle(\text{C}_\alpha-\text{C}_m-\text{H}_2) + \angle(\text{C}_\alpha-\text{C}_m-\text{H}_3)]/3$	
$\angle(\text{C}_\alpha-\text{C}_m-\text{H})_{\text{Diff1}} = 2[\angle(\text{C}_\alpha-\text{C}_m-\text{H}_1)] - \angle(\text{C}_\alpha-\text{C}_m-\text{H}_2) - \angle(\text{C}_\alpha-\text{C}_m-\text{H}_3)$	
$\angle(\text{C}_\alpha-\text{C}_m-\text{H})_{\text{Diff2}} = \angle(\text{C}_\alpha-\text{C}_m-\text{H}_2) - \angle(\text{C}_\alpha-\text{C}_m-\text{H}_3)$	

^a Distances in Å, angles in deg. Boldface denotes parameters included in the least-squares fits. Note that in Fits 1 and 2, all hydrogen atoms were fully positioned by the constraints, whereas Fit 3 provided four internal coordinates involving hydrogen atoms. ^b Refer to Figure 1 for atom labels.

atoms may be difficult to fit and should be treated judiciously to avoid vibrational contamination of r_e^{SE} structures.

III.C. r_e^{SE} Structure of Ala-I. The semiexperimental structures of **Ala-I** resulting from three different least-squares refinements, labeled Fit 1 through Fit 3, are reported in Table 3, along with the associated frozen-core CCSD(T)/cc-pVTZ r_e^{BO} parameters/constraints. The values refined in each fit are highlighted in boldface type with standard errors in parentheses, whereas all other parameters necessary to define the molecular structure were constrained to the CCSD(T)/cc-pVTZ values listed in normal type. In Fit 1 only the rotational constants of the parent and isotopologues involving heavy-atom substitution were used; accordingly, all hydrogen atoms were fully positioned by the r_e^{BO} constraints. By omitting the deuterated species, the errors in the B_e^{SE} data arising from large-amplitude vibrational effects are reduced and become more systematic. In Fit 1, the weighted root-mean-square (rms) residual of the 15 chosen rotational constants is only 16 kHz, and the standard errors of the fit for bond distances and angles are no greater than 0.007 Å and 0.6°, respectively. Clearly, the rotational constants of the parent, the ¹⁵N, and

the three unique ¹³C isotopologues provide enough information to determine the positions of all heavy atoms in **Ala-I**. Nonetheless, even in the highly constrained Fit 1 some of the optimized parameters are strongly correlated, hindering their explicit determination. The introduction of further constraints, for example fixing either $r(\text{C}-\text{O})$ or $r(\text{C}=\text{O})$, gave similar results. We note that the standard deviations of the r_e^{SE} (Fit 1) parameters are underestimations because the uncertainty of the several fixed parameters is not taken into account.

Fit 2 employed the same structural variables and constraints as Fit 1 but added selected rotational constants from the deuterated isotopologues to the B_e^{SE} data set. In particular, Fit 2 included $A_e^{\text{SE}}(\text{C}_\alpha-\text{D})$, $B_e^{\text{SE}}(\text{C}_m-3\text{D})$, $B_e^{\text{SE}}(\text{O}-\text{D})$, $C_e^{\text{SE}}(\text{O}-\text{D})$, $A_e^{\text{SE}}(\text{N}-\text{D}_b)$, and $C_e^{\text{SE}}(\text{N}-\text{D}_b)$, all of which had a residual <0.5 MHz in Fit 1. Fit 2 reduces the standard error of each structural parameter (Table 3) vis-à-vis Fit 1, while maintaining a reasonably small residual (24 kHz).

Fit 3 incorporated all of the observed rotational constants except those for the C_m-3D and $\text{N}-\text{D}_b$ isotopologues; in addition, $B_e^{\text{SE}}(\text{N}-\text{D}_a)$ was excluded and the weight of

$r_c^{\text{SE}}(\text{N}-\text{D}_a)$ was decreased, making the $\text{N}-\text{D}_a$ isotopologue less influential in the fit. Problems with nonsystematic errors necessitating exclusion of rotational constant data for the C_m-3D , $\text{N}-\text{D}_b$, and $\text{N}-\text{D}_a$ isotopologues were identified in section III.B above. The expanded data set for Fit 3 allowed some hydrogen-atom coordinates to be refined, the tightest fit to the data (weighted rms of 25 kHz) being obtained by releasing $r(\text{N}-\text{H})_{\text{Avg}}$, $\angle(\text{C}-\text{C}_\alpha-\text{H})$, $\angle(\text{C}-\text{O}-\text{H})$, and $\tau(\text{O}-\text{C}-\text{C}_\alpha-\text{H})$. Additional parameters could not be refined without introducing large deviations in both hydrogen- and heavy-atom positions. In this regard the structures of the methyl and carboxyl groups are under-determined by the experimental data, due to the lack of isotopic substitution on the oxygen atoms and on individual methyl hydrogen atoms. In summary, Fit 3 provides the best currently possible r_c^{SE} structure of **Ala-I** by refining 15 of the 33 geometric degrees of freedom on 23 vibrationally corrected, semiexperimental equilibrium rotational constants.

III.D. r_c^{SE} Structure of Ala-IIA. One satisfactory fit was achieved for the semiexperimental structure of **Ala-IIA**. Initially, incorporating only rotational constants of heavy-atom isotopologues and structural parameters involving heavy-atom positions, as in Fit 1 of **Ala-I**, resulted in an r_c^{SE} structure that had surprisingly large standard errors and poor agreement with the CCSD(T)/cc-pVTZ r_c^{BO} parameters. Most notably, the semiexperimental C–O distance had a standard error of 0.02 Å and was 0.04 Å shorter than the CCSD(T)/cc-pVTZ value, while the fit to the ^{15}N data was poor. As mentioned above, the ^{15}N assignments and the fitted data appear to be correct, but the originally reported and refitted uncertainties are probably too optimistic. Therefore, the structure of **Ala-IIA** was determined again after increasing the experimental uncertainties (reciprocal weights in the least-squares fit) of the three ^{15}N rotational constants by a factor of 20. This modification, labeled Fit 1', was validated by an approximate one-half reduction in the standard errors of the structural parameters. The C–O bond distance displayed an error of ± 0.01 Å and became a much more reasonable 0.01 Å shorter than the r_c^{BO} value. The final structural parameters of **Ala-IIA** refined in Fit 1' are reported in boldface in Table 4, along with the CCSD(T)/cc-pVTZ constraints invoked. While the success of the **Ala-IIA** fit is gratifying, the statistical errors are significantly larger than observed for Fit 1 of **Ala-I**.

Attempts to incorporate rotational constants of the deuterated isotopologues in the structural refinement of **Ala-IIA** did not reduce the statistical errors. Including the only two rotational constants that had residuals under 0.5 MHz in Fit 1' did not improve the heavy-atom structural parameters, unlike Fit 2 of **Ala-I**. Fitting the data for the $\text{C}_\alpha-3\text{D}$ and $\text{N}-\text{D}_a$ isotopologues once again proved problematic. Adding the O–D rotational constants and releasing the $\angle(\text{C}-\text{O}-\text{H})$ parameter distorted the **Ala-IIA** structure considerably, causing the carbonyl bond distance to deviate from the r_c^{BO} value by an unacceptable 0.1 Å. Other parameters for the hydroxyl hydrogen atom were released with similar or more pronounced distortion of the overall structure. Therefore, the B_c^{SE} data for the O–D isotopologue are disappointingly unable to yield the structure within the

Table 4. Equilibrium Structures of **Ala-IIA**^a

parameters ^b	CCSD(T)/cc-pVTZ	semiexperimental r_e (Fit 1')	
$r(\text{C}-\text{C}_\alpha)$	1.5347	1.530(3)	
$r(\text{C}_\alpha-\text{C}_m)$	1.5282	1.529(4)	
$r(\text{C}_\alpha-\text{N})$	1.4726	1.460(4)	
$r(\text{C}=\text{O})$	1.2052	1.205(9)	
$r(\text{C}-\text{O})$	1.3431	1.33(1)	
$\angle(\text{C}-\text{C}_\alpha-\text{C}_m)$	108.08	108.2(3)	
$\angle(\text{C}-\text{C}_\alpha-\text{N})$	109.44	109.8(4)	
$\angle(\text{C}_\alpha-\text{C}=\text{O})$	122.66	122.0(8)	
$\angle(\text{O}-\text{C}=\text{O})$	123.27	123.2(4)	
$\tau(\text{O}-\text{C}-\text{C}_\alpha-\text{C}_m)$	257.77	254.5(4)	
$\tau(\text{O}=\text{C}-\text{C}_\alpha-\text{N})$	195.28	192.5(5)	

CCSD(T)/cc-pVTZ r_e^{BO} constraints			
$r(\text{O}-\text{H})$	0.9789	$\angle(\text{C}_\alpha-\text{C}_m-\text{H})_{\text{Avg}}$	110.18
$r(\text{C}_\alpha-\text{H})$	1.0926	$\angle(\text{C}_\alpha-\text{C}_m-\text{H})_{\text{Diff1}}$	-0.60
$r(\text{N}-\text{H})_{\text{Avg}}$	1.0132	$\angle(\text{C}_\alpha-\text{C}_m-\text{H})_{\text{Diff2}}$	-0.33
$r(\text{N}-\text{H})_{\text{Diff}}$	0.0009	$\tau(\text{O}-\text{C}-\text{C}_\alpha-\text{H})$	140.31
$r(\text{C}_m-\text{H})_{\text{Avg}}$	1.0915	$\tau(\text{O}=\text{C}-\text{O}-\text{H})$	178.18
$r(\text{C}_m-\text{H})_{\text{Diff1}}$	-0.0067	$\tau(\text{C}_\alpha-\text{C}-\text{O}-\text{H})$	-4.10
$r(\text{C}_m-\text{H})_{\text{Diff2}}$	0.0005	$\tau(\text{C}-\text{C}_\alpha-\text{N}-\text{H}_a)$	89.86
$\angle(\text{C}-\text{O}-\text{H})$	104.26	$\tau(\text{C}-\text{C}_\alpha-\text{N}-\text{H}_b)$	208.10
$\angle(\text{C}-\text{C}_\alpha-\text{H})$	106.67	$\tau(\text{H}-\text{C}_\alpha-\text{C}_m-\text{H}_1)$	60.01
$\angle(\text{H}_a-\text{N}-\text{H}_b)$	106.90	$\tau(\text{H}-\text{C}_\alpha-\text{C}_m-\text{H}_2)$	179.80
$\angle(\text{C}-\text{N}-\text{H})_{\text{Avg}}$	110.61	$\tau(\text{H}-\text{C}_\alpha-\text{C}_m-\text{H}_3)$	-60.14

^a Distances in Å, angles in deg. Boldface denotes parameters included in the least-squares fits. Note that in Fit 1' all hydrogen atoms were fully positioned by the constraints. ^b Refer to Figure 1 for atom labels and Table 3 for coordinate definitions.

strong $\text{OH}\cdots\text{N}$ hydrogen bond. In summary, only the experimental rotational constants of the heavy-atom isotopologues yield useful information, and thus the r_c^{SE} structure of **Ala-IIA** is considerably less well determined than that of **Ala-I**.

III.E. Discussion of the Ala Structures. A comparison of prior experimental r_g , r_α , r_z , r_0 , and r_s parameters with the current r_c^{SE} and r_c^{BO} results is made in Tables 5 and 6 for **Ala-I** and **Ala-IIA**, respectively. Considerable vibrational effects are present in all previous experimental structures, and several structural parameters exhibit disturbing differences. The disparities are more prominent for the bond distances than for the bond angles. Our equilibrium r_c^{SE} and r_c^{BO} results allow unphysical or misleading values to be identified among the vibrationally averaged parameters. The most important defects are $r_g(\text{C}_\alpha-\text{C}_m) = 1.509(16)$ Å and $r_s(\text{C}_\alpha-\text{C}_m) = 1.57(1)$ Å compared to $r_c^{\text{SE}}(\text{C}_\alpha-\text{C}_m) = 1.522(4)$ Å for **Ala-I**; $r_0(\text{C}-\text{O}) = 1.37(2)$ Å compared to $r_c^{\text{SE}}(\text{C}-\text{O}) = 1.33(1)$ Å for **Ala-IIA**; and $r_s(\text{C}_\alpha-\text{N}) = 1.430(9)$ Å compared to $r_c^{\text{SE}}(\text{C}_\alpha-\text{N}) = 1.460(4)$ Å for **Ala-IIA**. Excessive deviations from the r_c^{SE} and r_c^{BO} values and underestimated experimental uncertainties are exhibited in several cases, such as $r_s(\text{C}_\alpha-\text{C}_m)$ of **Ala-IIA**, while anomalous vibrationally averaged distances smaller than the corresponding equilibrium bond length occur in other instances such as $r_z(\text{C}-\text{O})$ of **Ala-I**.

Several systematic studies^{84–87} have established the expected accuracy of CCSD(T)/cc-pVTZ geometric parameters, allowing a reliable assessment of our r_c^{BO} and r_c^{SE} structures of alanine. For 19 small (H, C, N, O, F) molecules, all-electron CCSD(T)/cc-pVTZ equilibrium bond distances have a mean error (std. dev.) of +0.0002 (0.0023) Å, whereas

Table 5. Selected **Ala-I** Structural Parameters (Å and deg) from Different Methodologies

	r_g/r_α ref 11 ^a	r_z ref 12	r_0 ref 5	r_s ref 5	r_e^{SE} Fit 3	r_e^{BO} CCSD(T)/cc-VTZ
$r(\text{C}-\text{C}_\alpha)$	1.544(10)	1.527(11)	1.51(1)	1.48(1)	1.520(3)	1.5236
$r(\text{C}_\alpha-\text{C}_\text{m})$	1.509(16)	1.536(11)	1.53(2)	1.57(1)	1.522(4)	1.5316
$r(\text{C}_\alpha-\text{N})$	1.471(7)	1.453(2)	1.45(1)	1.438(9)	1.448(4)	1.4570
$r(\text{C}=\text{O})$	1.192(2)	1.197(1)	1.24(2)		1.207(7)	1.2085
$r(\text{C}-\text{O})$	1.347(3)	1.341(2)	1.33(2)		1.349(6)	1.3551
$\angle(\text{C}-\text{C}_\alpha-\text{C}_\text{m})$	111.6(11)	111.9(2)	108.3(6)	109(1)	109.0(3)	108.70
$\angle(\text{C}-\text{C}_\alpha-\text{N})$	110.1(8)	112.9(3)	115(1)	117(1)	113.3(4)	113.24
$\angle(\text{C}_\alpha-\text{C}=\text{O})$	125.6(7)	125.7(3)	125(2)		125.1(4)	125.36
$\angle(\text{C}_\alpha-\text{C}-\text{O})$	110.3(7)	110.3(2)	113(2)			111.82
$\tau(\text{O}=\text{C}-\text{C}_\alpha-\text{N})$	-17.2(18)	-16.6(4)			-16.2(8)	-17.27

^a r_g for distances, r_α for angles.

Table 6. Selected **Ala-IIA** Structural Parameters (Å and deg) from Different Methodologies

	r_0 ref 5	r_s ref 5	r_e^{SE} Fit 1'	r_e^{BO} CCSD(T)/cc-VTZ
$r(\text{C}-\text{C}_\alpha)$	1.524(7)	1.517(7)	1.530(3)	1.5347
$r(\text{C}_\alpha-\text{C}_\text{m})$	1.543(8)	1.571(9)	1.529(4)	1.5282
$r(\text{C}_\alpha-\text{N})$	1.458(9)	1.430(9)	1.460(4)	1.4726
$r(\text{C}=\text{O})$	1.20(2)		1.205(9)	1.2052
$r(\text{C}-\text{O})$	1.37(2)		1.33(1)	1.3431
$\angle(\text{C}-\text{C}_\alpha-\text{C}_\text{m})$	107.1(3)	107.6(8)	108.2(3)	108.08
$\angle(\text{C}-\text{C}_\alpha-\text{N})$	111.7(7)	111.8(7)	109.8(4)	109.44
$\angle(\text{C}_\alpha-\text{C}=\text{O})$	125(1)		122.0(8)	122.66
$\angle(\text{C}_\alpha-\text{C}-\text{O})$	113(2)			114.02
$\tau(\text{O}=\text{C}-\text{C}_\alpha-\text{N})$	167(1)		192.5(5)	195.28

bond angles have a mean absolute error (MAE) of about 0.5° .⁸⁵ A very favorable cancellation of basis set incompleteness and electron correlation errors is responsible for such high accuracy. Statistics are not available for dihedral angles, but a larger MAE of perhaps $1-2^\circ$ is probable. Because 1s electron correlation contracts bond lengths in first-row diatomics by $0.0005-0.0025$ Å,^{55,88} frozen-core CCSD(T)/cc-pVTZ r_e^{BO} distances are expected to be too large by at least $0.001-0.003$ Å. Therefore, the general $r_e^{\text{BO}} > r_e^{\text{SE}}$ trend for bond distances in Tables 3 and 4 is nicely explained.

An investigation of 18 small, rigid molecules⁸⁹ showed that the MAE in the relative magnitude of the sum of theoretical α_i constants, $\sum_i \alpha_i^{\text{B}}/B_0$, was only 0.225% at the MP2/cc-pVDZ level of theory with respect to CCSD(T)/cc-pVQZ benchmarks. The resulting MAE for r_e^{SE} distances was a mere 0.0005 Å. Because our MP2/6-31G(d) α_i constants were computed with a basis set comparable to cc-pVDZ, electronic structure errors in the $B_e - B_0$ VPT2 vibrational corrections are not expected to have an appreciable effect on our r_e^{SE} results for Ala. An important caveat to this conclusion is that the test molecules of ref 89 did not have the troublesome, large-amplitude vibrational modes present in the alanine conformers. Nonetheless, the largest sources of error in the r_e^{SE} parameters are the modeling of vibrational effects via VPT2 theory, the phenomenological nature of the underlying empirical rotational constants, and the gaps in the isotopologic data. Taking into account all sources of error in both the theoretical and semiexperimental methods, the agreement in Tables 3 and 4 between the r_e^{BO} and r_e^{SE} structures of **Ala-I** and **Ala-IIA** is quite satisfactory. The dihedral angle $\tau(\text{O}=\text{C}-\text{C}_\alpha-\text{N})$ in **Ala-I** is a notable point of accord.

The conformational change from **Ala-I** to **Ala-IIA** yields considerable shifts in a few bond distances and angles.

Particularly prominent is the shift of the semiexperimental $\angle(\text{C}-\text{C}_\alpha-\text{N})$ angle from $113.3(4)^\circ$ in **Ala-I** to $109.8(4)^\circ$ in **Ala-IIA**, consistent with the trans-angle rule⁹⁰ of hyperconjugative and steric effects. In the r_s structures,⁵ there is also a large **Ala-I-Ala-IIA** difference in this angle, but the shift is overestimated, and $\angle(\text{C}-\text{C}_\alpha-\text{N})$ is much too large for both conformers. The carbonyl oxygen is involved in a bifurcated hydrogen bond in **Ala-I** but is uncomplexed in **Ala-IIA**. In both the r_e^{SE} and r_e^{BO} structures, the hydrogen bond formation is accompanied by an expected lengthening of $r(\text{C}=\text{O})$ by $0.002-0.003$ Å. While the r_0 structures⁵ exhibit $\text{C}=\text{O}$ bond elongation, the magnitude of the effect is $0.04(3)$ Å, a severe overestimation.

A key measure of the intramolecular hydrogen bonding in the Ala conformers is the associated heavy-atom distance $R(\text{N}\cdots\text{O})$. In the **Ala-I** [r_e^{SE} , r_e^{BO}] structures, $R(\text{N}\cdots\text{O}) = [2.825(12), 2.841]$ Å, while the corresponding values for **Ala-IIA** are $R(\text{N}\cdots\text{O}) = [2.605(18), 2.607]$ Å. Values for $R(\text{N}\cdots\text{O})$ hydrogen-bond distances computed at several levels of electronic structure theory are presented in Table S3 of the Supporting Information. The variations among the results demonstrate that our CCSD(T)/cc-pVTZ r_e^{BO} values for $R(\text{N}\cdots\text{O})$ should be accurate to ± 0.01 Å or better. **Ala-IIA** exhibits a larger, 0.034 Å discrepancy between the r_e^{SE} and r_e^{BO} H-bond lengths because of the aforementioned difficulty in determining the nitrogen-atom position. Likewise, both $\tau(\text{O}=\text{C}-\text{C}_\alpha-\text{N})$ and $r(\text{C}_\alpha-\text{N})$ of **Ala-IIA** significantly stray from the respective r_e^{BO} values. The much shorter $R(\text{N}\cdots\text{O})$ distance in **Ala-IIA** correctly reflects the greater strength of the $\text{OH}\cdots\text{N}$ hydrogen bond in this conformer compared to the $\text{NH}\cdots\text{O}$ bifurcated hydrogen bonds in **Ala-I**. Despite these relative hydrogen bond strengths, **Ala-I** is lower in energy than **Ala-IIA**, as definitively shown in section III.G below. The compensating energetic factor is the ~ 5 kcal mol⁻¹ more favorable (cis) arrangement of the carboxyl group in **Ala-I**.

III.F. Comparison of Ala and Gly Structures. A profitable comparison of the structures of the two simplest amino acids is afforded by our determination of the first r_e^{SE} parameters for **Ala-I** and **Ala-IIA** combined with analogous r_e^{SE} results for **Gly-Ip** and **Gly-IIn** from our earlier work.²⁴ The **Ala-I-GlyIp** differences in the heavy-atom bond distances are $\Delta r(\text{C}-\text{C}_\alpha) = +0.009$, $\Delta r(\text{C}_\alpha-\text{N}) = +0.007$, $\Delta r(\text{C}=\text{O}) = 0.000$, and $\Delta r(\text{C}-\text{O}) = -0.004$ Å, while the corresponding **Ala-IIA-GlyIIn** differences are $\Delta r(\text{C}-\text{C}_\alpha) = +0.006$, $\Delta r(\text{C}_\alpha-\text{N}) = -0.002$, $\Delta r(\text{C}=\text{O}) = +0.003$, and

Table 7. Focal Point Analysis of the **Ala-IIA–Ala-I** Energy Difference (kJ mol⁻¹)^a

	$\Delta E_e(\text{RHF})$	$\delta[\text{MP2}]$	$\delta[\text{CCSD}]$	$\delta[\text{CCSD(T)}]$	$\Delta E_e[\text{CCSD(T)}]$
aug-cc-pVDZ	10.81	-10.73	+2.63	-1.57	+1.14
aug-cc-pVTZ	10.50	-11.26	+2.86	-1.74	+0.35
aug-cc-pVQZ	10.51	-11.28	+2.97	[-1.74]	+0.46
aug-cc-pV5Z	10.54	-11.25	[+2.97]	[-1.74]	+0.52
CBS	[10.56]	[-11.21]	[+2.97]	[-1.74]	[+0.58]
extrapolation	$a + be^{-cX}$ ($X = 3, 4, 5$)	$a + bX^{-3}$ ($X = 4, 5$)	additive	additive	

$$\Delta E_0(\text{final}) = \Delta E_e[\text{CCSD(T)/CBS}] + \Delta_{\text{core}}[\text{CCSD(T)/cc-pCVTZ}] + \Delta_{\text{ZPVE}}[\text{MP2/aug-cc-pVTZ (pared)}] = +0.58 - 0.13 + 1.66 = \mathbf{2.11} \text{ kJ mol}^{-1}$$

^a The symbol δ denotes the increment in the relative energy (ΔE_e) with respect to the preceding level of theory in the hierarchy RHF \rightarrow MP2 \rightarrow CCSD \rightarrow CCSD(T). Square brackets signify results obtained from basis set extrapolations or additivity assumptions. Final predictions are boldfaced.

$\Delta r(\text{C}-\text{O}) = -0.003 \text{ \AA}$. Among these small changes, only the $\Delta r(\text{C}-\text{C}_\alpha)$ shifts are clearly significant compared to the uncertainty of the r_c^{SE} parameters. Likewise, the only significant change among the bond angles of the Gly and Ala heavy-atom frameworks occurs for $\angle(\text{C}-\text{C}_\alpha-\text{N})$, whose **Ala-I–GlyIp** and **Ala-IIA–GlyIn** shifts are -2.1° and -1.6° , respectively. Therefore, the main differences between the bond distances and angles in Gly and Ala are highly localized at the site of the methyl substitution.

The torsion angle $\tau(\text{O}=\text{C}-\text{C}_\alpha-\text{N})$ characterizes the deviation of the amino acid backbone from planarity. In **Gly-Ip** this angle is zero because the molecule has a symmetrical bifurcated hydrogen bond and adopts C_s point-group symmetry. Substitution of the methyl group in Ala breaks this symmetry significantly and leads to a torsion angle of $16.2(8)^\circ$ in **Ala-I**. In contrast, the backbones of **Gly-In** and **Ala-IIA** exhibit $\tau(\text{O}=\text{C}-\text{C}_\alpha-\text{N})$ angles of $11(2)^\circ$ and $12.5(5)^\circ$, respectively, which are essentially equivalent within the given uncertainties.

III.G. Relative Energy of Ala Conformers. The focal-point analysis of the energy of **Ala-IIA** relative to **Ala-I** (ΔE_e) is presented in Table 7. Showing rapid convergence to the CBS limit, the RHF relative energy and the MP2 correlation increment are converged to better than 0.1 kJ mol^{-1} using the aug-cc-pVTZ basis set. Basis sets with diffuse functions were employed specifically to treat the hydrogen bonding interactions.

The electron correlation sequence for ΔE_e shows less rapid convergence than the atomic-orbital basis set series. As seen in earlier studies,^{1,7,14} Hartree–Fock theory proves unreliable for conformational energetics of amino acids, placing **Ala-IIA** above **Ala-I** by a substantial $10.56 \text{ kJ mol}^{-1}$. The MP2 correlation energy largely rectifies this overestimation, but in the CBS limit, MP2 erroneously predicts that **Ala-IIA** is 0.65 kJ mol^{-1} lower in energy than **Ala-I**. With more sophisticated treatments of electron correlation, **Ala-I** is restored as the lowest energy conformer. The final frozen-core result is $\Delta E_e[\text{CCSD(T)/CBS}] = +0.58 \text{ kJ mol}^{-1}$, and appending the effect of core electron correlation (Δ_{core}), we obtain $\Delta E_e = +0.45 \text{ kJ mol}^{-1}$. The incorporation of connected quadruple excitations in coupled-cluster wave functions is not currently feasible for alanine, but several benchmark studies^{48,91–97} have shown that $\delta[\text{CCSDT(Q)}]$ relative-energy increments are typically about an order of magnitude smaller than $\delta[\text{CCSD(T)}]$ values. Therefore, considering all sources of error, our final equilibrium energy

difference is $\Delta E_e = +0.5(3) \text{ kJ mol}^{-1}$, in which the uncertainty estimate represents a 95% confidence interval.

Zero-point vibrational energy (ZPVE) increases the **Ala-IIA–Ala-I** energy separation by 1.66 kJ mol^{-1} , yielding $\Delta E_0 = +2.1(3) \text{ kJ mol}^{-1}$. Thus, ZPVE effects constitute almost 80% of the energy difference at 0 K. The low-frequency vibrational modes that were problematic in the r_c^{SE} analysis do not appear to add significant uncertainty to the ΔE_0 determination, as less than 1% of the ZPVE effect arises from anharmonic corrections.

IV. Summary

This investigation is the first to conjoin theory and experiment to not only determine reliable semiexperimental r_c structures (r_c^{SE}) for conformers of a molecule as large and flexible as alanine (Ala) but also to analyze in detail the factors contributing to the accuracy of such parameters. It is shown convincingly that an accurate r_c^{SE} structure for a flexible molecule can indeed be determined if procedures developed for (semi)rigid systems are carefully employed. For alanine, we find that the outcome of the r_c^{SE} least-squares refinement depends critically on the accuracy of the equilibrium rotational constants, as expected, as well as the attendant uncertainties, which is less expected. Therefore, our study commenced by refitting all the spectroscopic constants of **Ala-I** and **Ala-IIA** to the experimentally measured rotational transitions to ensure a dependable reference data set. A predicate observations scheme using ab initio quartic centrifugal distortion information appears to work well even for such a flexible molecule. In refining r_c^{SE} structures for Ala, we discovered that not all effective rotational constants can be utilized, even if their apparent uncertainty is small. The problem results mostly from the effective nature of the empirical rotational constants and, to a lesser extent, from limitations of the theoretical vibration–rotation interaction treatment. It is essential to constrain the r_c^{SE} fit using accurate Born–Oppenheimer equilibrium (r_c^{BO}) parameters, obtained here at the frozen-core CCSD(T)/cc-pVTZ level of electronic structure theory. A proper choice of the fitted and constrained parameters is paramount to obtaining good r_c^{SE} results. In general, the heavy-atom positions are well determined by the fits, whereas the hydrogen atoms must be constrained. Avoiding overfitting requires particular attention to statistical details.

The r_c^{SE} parameters determined in this study demonstrate that vibrational effects *must* be removed to get meaningful

structures for large and flexible systems from rotational constants. Specifically, previous vibrationally averaged r_g / r_a , r_z , r_0 , and r_s structures for Ala are shown to be defective, exhibiting errors as large as 0.04 Å for bond distances, 3° for bond angles, and 25° for torsion angles. Therefore, small and intrinsic conformation-induced changes are reliably discerned only when precise r_e structures are known, because vibrational effects can mask the true variations. Our r_e^{SE} results are significant in this regard because they provide the first sound comparison of empirically based structures for the two simplest amino acids, Gly and Ala.

Through convergent focal-point analysis (FPA) ab initio computations, the energy difference between the lowest conformers of alanine has been pinpointed for the first time, proving that **Ala-I** and **Ala-IIA** are almost isoenergetic. The **Ala-IIA** equilibrium structure is higher in energy than that of **Ala-I** by a mere 0.5(3) kJ mol⁻¹, and with inclusion of zero-point vibrational energy (ZPVE), this relative energy is still only 2.1(3) kJ mol⁻¹. Our high-level computations also reveal that the unobserved **Ala-IIB** conformer has a tenuous existence as a distinct species, being separated from **Ala-IIA** by a vibrationally adiabatic isomerization barrier less than 0.2 kJ mol⁻¹.

Much attention has been afforded glycine and alanine as essential origin-of-life molecules, and as such, their existence in interstellar space has been actively researched. Until now, only a few molecules of possible biochemical interest have been detected with certainty in interstellar environments: glycolaldehyde, a small “sugar”;⁹⁸ acetamide, a molecule with a peptide bond;⁹⁹ and aminoacetonitrile, a precursor of glycine.¹⁰⁰ Glycine has been detected only tentatively.^{101,102} The difficulties of detecting glycine may be explained partly by the small dipole-moment components of its most stable conformer (**Gly-Ip**), for example, $\mu_a = 0.91$ D.¹⁰³ In contrast, for **Ala-I** the μ_b dipole component has been measured to be 1.6 D.⁹ The present study confirms unequivocally that **Ala-I** is the most stable form of α -alanine and supports the somewhat imprecise dipole moment measurements of Godfrey et al.⁹ Because b -type transitions have larger line strengths than a -type transitions, the μ_b component of **Ala-I** might be large enough to permit the interstellar detection of α -alanine, provided it is sufficiently abundant in the source. The interplay of theory and experiment could prove very productive toward this goal.

Acknowledgment. Dr. Steven Wheeler is thanked for helpful discussions. The research in Athens at the University of Georgia was supported by the U.S. National Science Foundation, Grant CHE-0749868. The work performed in Hungary and the Athens/Budapest collaboration received support from the Hungarian Scientific Research Fund, OTKA K72885 and IN77954, respectively. The joint work between Lille and Budapest was partially supported by EGIDE. The high-accuracy ab initio computations used resources of the National Energy Research Scientific Computing Center (NERSC), which is supported by the Office of Science of the U.S. Department of Energy under Contract No. DE-AC02-05CH11231.

Supporting Information Available: Cartesian coordinates of CCSD(T)/cc-pVTZ equilibrium structures; refit (A_0 , B_0 , C_0) and semiexperimental (A_e , B_e , C_e) rotational constants for **Ala-I** and **Ala-IIA** isotopologues; hydrogen-bond distances $R(\text{N}\cdots\text{O})$ for various levels of theory, and complete refs 60 and 61. This material is available free of charge via the Internet at <http://pubs.acs.org>.

References

- (1) Császár, A. G.; Perczel, A. *Prog. Biophys. Mol. Biol.* **1999**, *71*, 243.
- (2) Dian, B. C.; Clarkson, J. R.; Zwier, T. S. *Science* **2004**, *303*, 1169.
- (3) Robertson, E. G.; Simons, J. P. *Phys. Chem. Chem. Phys.* **2000**, *3*, 1.
- (4) Gronert, S.; O'Hair, R. A. J. *J. Am. Chem. Soc.* **1995**, *117*, 2071.
- (5) Blanco, S.; Lesarri, A.; Lopez, J. C.; Alonso, J. L. *J. Am. Chem. Soc.* **2004**, *126*, 11675.
- (6) Cao, M.; Newton, S. Q.; Pranata, J.; Schäfer, L. *J. Mol. Struct.* **1995**, *332*, 251.
- (7) Császár, A. G. *J. Phys. Chem.* **1996**, *100*, 3541.
- (8) Császár, A. G. *J. Mol. Struct.* **1994**, *346*, 141.
- (9) Godfrey, P. D.; Firth, S.; Hatherley, L. D.; Brown, R. D.; Pierlot, A. P. *J. Am. Chem. Soc.* **1993**, *115*, 9687.
- (10) Hirata, Y.; Kubota, S.; Watanabe, S.; Momose, T.; Kawaguchi, K. *J. Mol. Spectrosc.* **2008**, *251*, 314.
- (11) Iijima, K.; Beagley, B. *J. Mol. Struct.* **1991**, *248*, 133.
- (12) Iijima, K.; Nakano, M. *J. Mol. Struct.* **1999**, *486*, 255.
- (13) Stepanian, S. G.; Reva, I. D.; Radchenko, E. D.; Adamowicz, L. *J. Phys. Chem. A* **1998**, *102*, 4623.
- (14) Császár, A. G. *J. Am. Chem. Soc.* **1992**, *114*, 9568.
- (15) Maul, R.; Ortmann, F.; Preuss, M.; Hannewald, K.; Bechstedt, F. *J. Comput. Chem.* **2007**, *28*, 1817.
- (16) Rak, J.; Skurski, P.; Simons, J. P.; Gutowski, M. *J. Am. Chem. Soc.* **2001**, *123*, 11695.
- (17) Snoek, L. C.; Robertson, E. G.; Kroemer, R. T.; Simons, J. P. *Chem. Phys. Lett.* **2000**, *321*, 49.
- (18) Szidarovszky, T.; Czako, G.; Császár, A. G. *Mol. Phys.* **2009**, *107*, 761.
- (19) Wilke, J. J.; Lind, M. C.; Schaefer, H. F.; Császár, A. G.; Allen, W. D. *J. Chem. Theory Comput.* **2009**, *5*, 1511.
- (20) Godfrey, P. D.; Brown, R. D.; Rodgers, F. M. *J. Mol. Struct.* **1996**, *376*, 65.
- (21) Pulay, P.; Meyer, W.; Boggs, J. E. *J. Chem. Phys.* **1978**, *68*, 5077.
- (22) Botschwina, P.; Oswald, M.; Flugge, J.; Heyl, A.; Oswald, R. *Chem. Phys. Lett.* **1993**, *209*, 117.
- (23) Allen, W. D.; Czinki, E.; Császár, A. G. *Chem.—Eur. J.* **2004**, *10*, 4512.
- (24) Kasalová, V.; Allen, W. D.; Schaefer, H. F.; Czinki, E.; Császár, A. G. *J. Comput. Chem.* **2007**, *28*, 1373.
- (25) Thiel, W.; Scuseria, G.; Schaefer, H. F.; Allen, W. D. *J. Chem. Phys.* **1988**, *89*, 4965.

- (26) Breidung, J.; Cosleou, J.; Demaison, J.; Sarka, K.; Thiel, W. *Mol. Phys.* **2004**, *102*, 1827.
- (27) Cazzoli, G.; Cludi, L.; Contento, M.; Puzzarini, C. *J. Mol. Spectrosc.* **2008**, *251*, 229.
- (28) Demaison, J.; Császár, A. G.; Dehayem-Kamadjeu, A. *J. Phys. Chem. A* **2006**, *110*, 13609.
- (29) Demaison, J.; Lievin, J.; Császár, A. G. *J. Phys. Chem. A* **2008**, *112*, 4477.
- (30) Demaison, J.; Margules, L.; Maeder, H.; Sheng, M.; Rudolph, H. D. *J. Mol. Spectrosc.* **2008**, *252*, 169.
- (31) East, A. L. L.; Allen, W. D.; Klippenstein, S. J. *J. Chem. Phys.* **1995**, *102*, 8506.
- (32) East, A. L. L.; Johnson, C. S.; Allen, W. D. *J. Chem. Phys.* **1993**, *98*, 1299.
- (33) Gauss, J.; Stanton, J. F. *J. Phys. Chem. A* **2000**, *104*, 2865.
- (34) Gordon, V. D.; Nathan, E. S.; Apponi, A. J.; McCarthy, M. C.; Thaddeus, P.; Botschwina, P. *J. Chem. Phys.* **2000**, *113*, 5311.
- (35) Boese, A. D.; Martin, J. M. L.; Klopper, W. *J. Phys. Chem. A* **2007**, *111*, 11122.
- (36) Lane, J. R.; Kjaergaard, H. G. *J. Chem. Phys.* **2009**, *131*, 034307.
- (37) Paizs, B.; Salvador, P.; Császár, A. G.; Duran, M.; Suhai, S. *J. Comput. Chem.* **2001**, *22*, 196.
- (38) Sellers, H. L.; Schafer, L. *Chem. Phys. Lett.* **1979**, *63*, 609.
- (39) Allen, W. D.; East, A. L. L.; Császár, A. G., In *Structures and Conformations of Non-Rigid Molecules*; Laane, J., Dakkouri, M., van der Veeken, B., Oberhammer, H., Eds.; Kluwer: Dordrecht, The Netherlands, 1993; pp 343–373.
- (40) Császár, A. G.; Allen, W. D.; Schaefer, H. F. *J. Chem. Phys.* **1998**, *108*, 9751.
- (41) Császár, A. G.; Tarczay, G.; Leininger, M. L.; Polyansky, O. L.; Tennyson, J.; Allen, W. D. In *Spectroscopy from Space*, Demaison, J., Sarka, K., Eds.; Kluwer: Dordrecht, The Netherlands, 2001; pp 317–339.
- (42) East, A. L. L.; Allen, W. D. *J. Chem. Phys.* **1993**, *99*, 4638.
- (43) Gonzales, J. M.; Pak, C.; Cox, R. S.; Allen, W. D.; Tarczay, G.; Császár, A. G. *Chem.—Eur. J.* **2003**, *9*, 2173.
- (44) Schuurman, M. S.; Allen, W. D.; Schleyer, P. v. R.; Schaefer, H. F. *J. Chem. Phys.* **2005**, *122*, 104302.
- (45) Czakó, G.; Braams, B. J.; Bowman, J. M. *J. Phys. Chem. A* **2008**, *112*, 7466.
- (46) Schuurman, M.; Muir, S.; Allen, W. D.; Schaefer, H. F. *J. Chem. Phys.* **2004**, *120*, 11586.
- (47) Czakó, G.; Nagy, B.; Tasi, G.; Somogyi, A.; Šimunek, J.; Noga, J.; Braams, B. J.; Bowman, J. M.; Császár, A. G. *Int. J. Quantum Chem.* **2009**, *109*, 2393.
- (48) Simmonett, A. C.; Schaefer, H. F.; Allen, W. D. *J. Chem. Phys.* **2009**, *130*, 044301.
- (49) Wheeler, S. E.; Allen, W. D.; Schaefer, H. F. *J. Chem. Phys.* **2004**, *121*, 8800.
- (50) Wheeler, S. E.; Robertson, K. A.; Allen, W. D.; Schaefer, H. F.; Bomble, Y. T.; Stanton, J. F. *J. Phys. Chem. A* **2007**, *111*, 3819.
- (51) Bartlett, R. J.; Watts, J. D.; Kucharski, S. A.; Noga, J. *Chem. Phys. Lett.* **1990**, *165*, 513.
- (52) Bartlett, R. J.; Watts, J. D.; Kucharski, S. A.; Noga, J. *Chem. Phys. Lett.* **1990**, *167*, 609.
- (53) Raghavachari, K.; Trucks, G. W.; Pople, J. A.; Head-Gordon, M. *Chem. Phys. Lett.* **1989**, *157*, 479.
- (54) Dunning, T. H., Jr. *J. Chem. Phys.* **1989**, *90*, 1007.
- (55) Császár, A. G.; Allen, W. D. *J. Chem. Phys.* **1996**, *104*, 2746.
- (56) Fogarasi, G.; Zhou, X.; Taylor, P. W.; Pulay, P. *J. Am. Chem. Soc.* **1992**, *114*, 8191.
- (57) Pulay, P.; Fogarasi, G.; Pang, F.; Boggs, J. E. *J. Am. Chem. Soc.* **1979**, *101*, 2550.
- (58) Crawford, T. D.; Sherrill, C. D.; Valeev, E. F.; Fermann, J. T.; King, R. A.; Leininger, M. L.; Brown, S. T.; Janssen, C. L.; Seidl, E. T.; Kenny, J. P.; Allen, W. D. *J. Comput. Chem.* **2007**, *28*, 1610.
- (59) Dunning, T. H., Jr. *J. Chem. Phys.* **1970**, *53*, 2823.
- (60) Werner, H.-J. et al. *Molpro, A Package of Ab Initio Programs*, version 2006.1.
- (61) ACESII, J. F. Stanton et al. For current version, see <http://www.aces2.de>. See also Stanton, J. F.; Gauss, J.; Watts, J. D.; Lauderdale, W. J.; Bartlett, R. J. *Int. J. Quantum Chem. Symp.* **1992**, *26*, 879.
- (62) Francl, M. M.; Pietro, W. J.; Hehre, W. J.; Binkley, J. S.; Gordon, M. S.; Defrees, D. J.; Pople, J. A. *J. Chem. Phys.* **1982**, *77*, 3654.
- (63) Allen, W. D.; Császár, A. G. *J. Chem. Phys.* **1993**, *98*, 2983.
- (64) Stanton, J. F.; Lopreore, C. L.; Gauss, J. *J. Chem. Phys.* **1998**, *108*, 7190.
- (65) Mills, I. M., In *Molecular Spectroscopy: Modern Research*; Rao, K. N., Mathews, C. W., Eds.; Academic Press: New York, 1972; Vol. 1, pp 115–140.
- (66) Curl, R. F. *J. Comput. Phys.* **1970**, *6*, 367.
- (67) Gordy, W.; Cook, R. L. In *Microwave Molecular Spectra*; John Wiley & Sons: New York, 1984; Vol. 18, pp 647–724.
- (68) Lees, R. M. *J. Mol. Spectrosc.* **1970**, *33*, 124.
- (69) MolStruct is an abstract program developed by Wesley D. Allen for use within Mathematica (Wolfram Research Inc., Champaign, IL) to perform diverse fits of molecular structures to sets of isotopologic rotational constants.
- (70) Demaison, J. *Mol. Phys.* **2007**, *105*, 3109.
- (71) Kendall, R. A.; Dunning, T. H., Jr.; Harrison, R. J. *J. Chem. Phys.* **1992**, *96*, 6796.
- (72) Feller, D. *J. Chem. Phys.* **1993**, *98*, 7059.
- (73) Helgaker, T.; Klopper, W.; Koch, H.; Noga, J. *J. Chem. Phys.* **1997**, *106*, 9639.
- (74) Pared aug-cc-pVTZ basis set specifications: for the C, C α , N, and O atoms, aug-cc-pVTZ sans the diffuse f functions; for the amino and hydroxyl hydrogens, aug-cc-pVTZ sans the diffuse d functions; for C β , as well as the methyl and C α hydrogens, cc-pVTZ.
- (75) Felder, P.; Günthard, H. H. *Chem. Phys.* **1982**, *71*, 9.
- (76) Ruoff, R. S.; Klots, T. D.; Emilsson, T.; Gutowsky, H. S. *J. Chem. Phys.* **1990**, *93*, 3142.
- (77) Belsley, D. A. *Conditioning Diagnostics: Colinearity and Weak Data in Regression*; Wiley: Chichester, U.K., 1991.

- (78) Rousseeuw, P. J.; Leroy, A. M. *Robust Regression in Outlier Detection*; Wiley: New York, 1987.
- (79) Watson, J. K. G. In *Vibrational Spectra and Structure*; Durig, J. R., Ed. Elsevier: Amsterdam, 1977; pp 1–89.
- (80) Rudolph, H. D. Z. *Naturforsch.* **1968**, *23a*, 540.
- (81) Bartell, L. S.; Romanesko, D. J.; Wong, T. C. In *Molecular Structure by Diffraction Methods*; Sims, G. A., Sutton, L. E., Eds.; The Chemical Society: London, 1975; Vol. 3, p 72.
- (82) Császár, A. G.; Fogarasi, G. *J. Chem. Phys.* **1989**, *89*, 7647.
- (83) Wlodarczak, G.; Burie, J.; Demaison, J.; Vormann, K.; Császár, A. G. *J. Mol. Spectrosc.* **1989**, *134*, 297.
- (84) Demaison, J.; Herman, M.; Liévin, J. *Int. Rev. Phys. Chem.* **2007**, *26*, 391.
- (85) Bak, K. L.; Gauss, J.; Jørgensen, P.; Olsen, J.; Helgaker, T.; Stanton, J. F. *J. Chem. Phys.* **2001**, *114*, 6548.
- (86) Demaison, J.; Margulès, L.; Boggs, J. E. *Chem. Phys.* **2000**, *260*, 65.
- (87) Margulès, L.; Demaison, J.; Boggs, J. E. *J. Mol. Struct.* **2000**, *500*, 245.
- (88) Martin, J. M. L. *Chem. Phys. Lett.* **1995**, *242*, 343.
- (89) Pawlowski, F.; Jørgensen, P.; Olsen, J.; Hegelund, F.; Helgaker, T.; Gauss, J.; Bak, K. L.; Stanton, J. F. *J. Chem. Phys.* **2002**, *116*, 6482.
- (90) Rasanen, M.; Aspiala, A.; Homanen, L.; Murto, J. *J. Mol. Struct.* **1982**, *96*, 81.
- (91) Bomble, Y. J.; Vazquez, J.; Kállay, M.; Michauk, C.; Szalay, P. G.; Császár, A. G.; Gauss, J.; Stanton, J. F. *J. Chem. Phys.* **2006**, *125*, 064108.
- (92) Czako, G.; Mátyus, E.; Simmonett, A. C.; Császár, A. G.; Schaefer, H. F.; Allen, W. D. *J. Chem. Theory Comput.* **2008**, *4*, 1220.
- (93) Feng, H.; Allen, W. D. *J. Chem. Phys.* **2010**, *132*, 094304.
- (94) Simmonett, A. C.; Stibrich, N. J.; Papas, B. N.; Schaefer, H. F.; Allen, W. D. *J. Phys. Chem. A* **2009**, *113*, 11643.
- (95) Tajti, A.; Szalay, P. G.; Császár, A. G.; Kállay, M.; Gauss, J.; Valeev, E. F.; Flowers, B. A.; Vazquez, J.; Stanton, J. F. *J. Chem. Phys.* **2004**, *121*, 11599.
- (96) Wheeler, S. E.; Houk, K. N.; Schleyer, P. v. R.; Allen, W. D. *J. Am. Chem. Soc.* **2009**, *131*, 2547.
- (97) Wheeler, S. E.; Robertson, K. A.; Allen, W. D.; Schaefer, H. F.; Bomble, Y. J.; Stanton, J. F. *J. Phys. Chem. A* **2007**, *111*, 3819.
- (98) Hollis, J. M.; Jewell, P. R.; Lovas, F. J.; Remijan, A. *Astrophys. J. Lett.* **2004**, *613*, L45.
- (99) Hollis, J. M.; Lovas, F. J.; Remijan, A. J.; Jewell, P. R.; Ilyushin, V. V.; Kleiner, I. *Astrophys. J. Lett.* **2006**, *643*, L25.
- (100) Belloche, A.; Menten, K. M.; Comito, C.; Müller, H. S. P.; Schilke, P.; Ott, J.; Thorwirth, S.; Hieret, C. *Astron. Astrophys.* **2008**, *482*, 179.
- (101) Kuan, Y. J.; Charnley, S. B.; Huang, H. C.; Kisiel, Z. *Astrophys. J.* **2003**, *593*, 848.
- (102) Snyder, L. E.; Lovas, F. J.; Hollis, J. M.; Friedel, D. N.; Jewell, P. R.; Remijan, A.; Ilyushin, V. V.; Alekseev, E. A.; Dyubko, S. F. *Astrophys. J.* **2005**, *619*, 914.
- (103) Lovas, F. J.; Zobov, N.; Fraser, G. T.; Suenram, R. D. *J. Mol. Spectrosc.* **1995**, *171*, 189.

CT1000236